

1-D consolidation theory developed based on in-depth experimental findings

Hideki Ohta,

Research and Development Initiative, Chuo University, Tokyo, Japan, ohta@tamacc.chuo-u.ac.jp

Atsushi Iizuka

Research and Development Initiative, Chuo University, Tokyo, Japan

Yoshiyuki Morikawa

Port and Airport Research Institute, National Institute of Maritime, Port and Aviation Technology, Kanagawa, Japan

Kazuaki Uemura

Core-Labo Testing Center, Engineering Headquarters, OYO Corporation, Saitama, Japan

Tomohide Takeyama, Shinya Tachibana

Graduate School of Engineering, Kobe University, Hyogo, Japan

ABSTRACT: Ohta et al. (Proc. 20th ICSMGE, Sydney, 179–184, 2022) reported the results of an oedometer test on silty clay ($w_n = 57.57\%$) water content of which was reduced to 37.27% that was about 7% higher than the plastic limit ($w_p = 30.50\%$) through partial freeze-drying. It was indirectly proven that the micro-structure of the clay and pore water around clay particles remained the same before partial freeze-drying. No primary compression occurred, and secondary compression started immediately after applying the load, i.e. immediately after the instantaneous increase in the effective stress. The observed compressive strain continued to increase proportionally with the logarithm of elapsed time from the beginning of each loading step. It was also found that the compressive strain at the start of each loading step was the same as the final strain at the previous loading step, implying that the spring (represented by m_v) needed to derive Terzaghi's one-dimensional (1-D) consolidation equation should be replaced by a Voigt model, furnishing a spring and dash pot in parallel. In this study, oedometer tests are performed on 8 clay specimens ($w_L > 50\%$) taken from the seabed in the expansion area of Haneda Airport in Tokyo Bay. No instantaneous elastic response is observed, confirming the abovementioned conclusions. Based on these experimental findings, this study develops a new theory of 1-D consolidation. The basic equation $\partial p_w / \partial t = c_v (\partial^2 p_w) / (\partial z^2) + \alpha / (m_v t)$, $c_v = k / (\gamma_w m_v)$ is obtained, which furnishes the second term when compared with Terzaghi's basic equation. It is found that the equation $\partial \varepsilon / \partial t = c_v (\partial^2 \varepsilon) / (\partial z^2)$ independently proposed by McNabb (1960) and Mikasa (1963) can be derived from the basic equation shown above. Compared with Terzaghi's equation, the new equation provides an earlier slowdown of settlement and a slower dissipation of excess pore water pressure.

KEYWORDS: 1-D consolidation, creep, secondary compression, Terzaghi's theory, Mikasa's consolidation equation

1 INTRODUCTION

The entire process of compression of clay specimens in oedometer tests is traditionally divided into two stages: (i) the primary compression, in which the excess pore water pressure gradually dissipates with time (while the effective stress increases), and (ii) the secondary compression, in which the slower rate of compression continues under practically constant effective stress. In many cases, the compression observed in the secondary stage is considered as the viscous behaviour, i.e. creep, of clays. How do we estimate the contribution of creep compression during the primary compression? What would be a rational way to consider the effect of creep in estimating time-compression curves? This is a serious issue we have faced over the past 100 years. Owing to the intrinsic nature of primary compression, we have been unsuccessful in providing a direct answer supported by definitive experimental evidence. Ladd et al. (1977) concluded in their state-of-the-art report that little definitive data on this question.

In our engineering practice dealing with the one-dimensional (1-D) compression of a clay layer caused by an increment in uniform load, we use the Terzaghi theory to estimate the rate of dissipation of the excess pore water pressure. According to the Terzaghi theory, the consolidation of clays during the primary compression stage occurs owing to the instantaneous elastic (or elasto-plastic) response of clays to the increase in effective stress, accompanied by the gradual dissipation of excess pore water pressure. The time-dependent response of clays that causes the secondary compression stage

is more complex and has been interpreted using four different approaches:

- Rheological models of creep (or inelastic) response in addition to instantaneous elastic (or elasto-plastic) response: Taylor and Merchant (1940) and others
- Relationship between void ratio e , effective stress σ' , and loading duration: Taylor (1948), Bjerrum (1967), Garlanger, J. E. (1972)
- Relationship between void ratio e , effective stress σ' , and strain rate $\partial e / \partial t$: Suklje (1942), Hawley and Borin (1977), Imai (1989), Den Haan (1996), Yin (1996)
- Unique relationship between void ratio e and effective stress σ' at the end of primary (EOP): Mesri and Choi (1985)

The complexities in interpretation arise from the fact that oedometer tests on saturated clay specimens are not element tests but boundary value problems, in which clay elements behave differently depending on how far they are located from the drainage boundary. For this reason, the mechanical behaviour of each element (thin slice of clay) cannot be directly observed during the entire consolidation process unless the specimen is horizontally cut piecewise and connected in series to form a specimen of the intended thickness, such as that introduced by Mesri and Choi (1985) and Imai (1989). The time delay of compression observed in the primary compression stage is caused by the pore water slowly flowing out from macropores of clays. This retardation action of the outwards flow of pore water could be eliminated by removing the pore

water from macropores in the specimens subjected to oedometer tests. By employing partial freeze-drying, Ohta et al. (2022) were successful in removing a major part of pore water from the macropores without distorting the micro-structures of the clay ‘skeleton’ (allowing the double-layered water to remain stationary on the surface of clay particles). Through their experimental work, they observed the following:

- 1) No primary stage of compression occurred. Only the secondary compression that started immediately after applying the load was observed, i.e. immediately after an instantaneous increase in effective stress (because of the lack of pore water in macropores). The observed compressive strain continued to increase proportionally with the logarithm of elapsed time from the beginning of each loading step.
- 2) The compressive strain at the starting moment of each loading step was identical to the final strain at the previous loading step. This implies that the spring (represented by m_v) required to derive Terzaghi’s 1-D consolidation equation should be replaced by a Voigt model, furnishing a spring and dash pot in parallel.

2 EXPERIMENTAL EVIDENCE-I

In this paper, the term ‘primary compression’ is used vaguely, although it should be used to describe the consolidation process in which a unique relationship between the void ratio and effective stress is obeyed by the soil. On the other hand, the term ‘secondary compression’ is one in which this condition is not satisfied. (Definitions by Hawley and Borin, 1973)

The experimental work conducted by Ohta et al. (2022) is briefly described as follows. The creep compression before the completion of the primary compression is not observable conventionally because it is embedded in the primary compression. To observe the creep compression which may start developing immediately after loading, it is necessary to complete the primary compression very quickly, if possible, immediately after loading. This can be achieved by removing a major part of the pore water from macropores without distorting the micro-structures of the clay ‘skeleton’.

The freeze-drying technique is introduced to observe creep compression throughout the entire testing period. A partially freeze-dried specimen was produced by removing a major portion of the pore water from macropores of the specimen without activating the effect of the capillary force, while allowing the double-layered water to remain stationary on the surface of clay particles. Two specimens of Holocene silty clay (with specific gravity of soil particle $G_s = 2.690$, liquid limit $w_L = 59.70\%$, plastic limit $w_P = 30.50\%$) are cut out of an undisturbed sample collected from a depth of 14.0–14.8 m at Kita-Katsushika near the mouth of the Ara River flowing into Tokyo Bay in Japan. One of the two specimens, N (natural specimen, natural water content $w_n = 57.21\%$, void ratio $e = 1.539$, pre-consolidation pressure $p_c = 167.8 \text{ kN/m}^2$) is subjected to an oedometer test in the conventional way. The other specimen, D (partially freeze-dried specimen, natural water content $w_n = 57.54\%$, void ratio $e = 1.548$, pre-consolidation pressure $p_c = 154.0 \text{ kN/m}^2$) is partially freeze-dried (water content $w = 37.27\%$) and then subjected to an oedometer test. The water content of Specimen D decreased from $w_n = 57.54\%$ to $w = \text{plastic limit } (w_P = 30.50\%) + 8\%$ via the freeze-drying process. In preliminary tests, δ was chosen as approximately 7%. The sublimation of the pore water in the frozen specimen subjected to vacuum pressure in a desiccator is accelerated using a cold trap, in which the vaporised pore water is frozen again. The weight of Specimen

D in the drying process in a desiccator is measured at specific time intervals until the water content reaches the target.

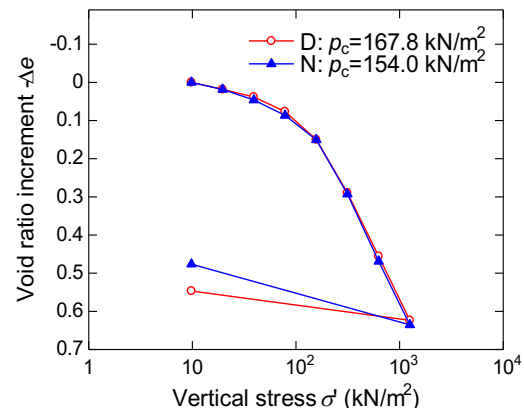


Figure 1 $\Delta e - \log \sigma'$ relations

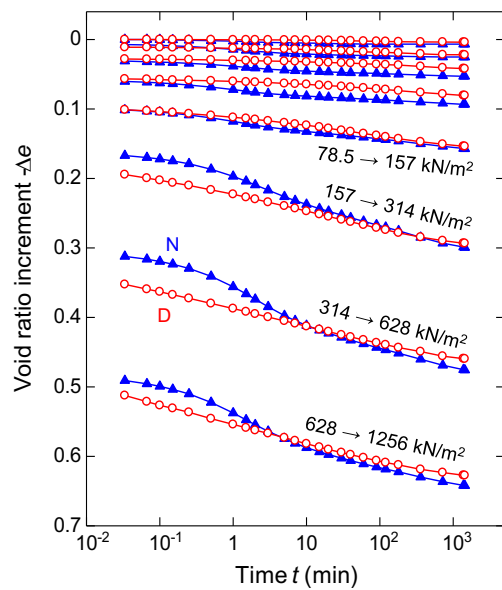


Figure 2 $\Delta e - \log t$ relationships

The $e - \log \sigma'$ plots of the oedometer tests on Specimens N and D are shown in Figure 1. They demonstrate that the micro-structure of the partially freeze-dried Specimen D is almost mechanically identical to that of Specimen N, which is not frozen. Figure 2 summarises the results of the oedometer tests on Specimens N and D. The decrease in the void ratio is plotted against $\log t$, where the data points of triangles (\blacktriangle) and circles (\circ) represent Specimens N and D, respectively. In the first five loading steps ($0 \rightarrow 9.8, 9.8 \rightarrow 19.6, 19.6 \rightarrow 39.2, 39.2 \rightarrow 78.5$ and $78.5 \rightarrow 157.0 \text{ kN/m}^2$), the specimens remain in an over-consolidated state, and primary compression is completed very quickly. In the subsequent three loading steps ($157 \rightarrow 314, 314 \rightarrow 628$, and $628 \rightarrow 1256 \text{ kN/m}^2$), in which the specimens are in normally consolidated states, the decrease in the void ratio of Specimen N (triangles \blacktriangle) is inhibited compared with that of Specimen D (circles \circ). This slow process of primary compression of Specimen N is caused by the slow speed of pore water flowing from macropores towards the outside.

The primary compression of Specimen N in normally consolidated states takes 10–30 min to be practically completed, as shown in Figure 2, while the secondary compression (creep) continued to occur until the end of each

loading step (1440 min after loading). The secondary compression curves of Specimen N in normally consolidated states approximately overlap with those of Specimen D, which are nearly linear when plotted against the logarithm of elapsed time t . A major part of the volume of macropores in Specimen D was occupied by air, which can be instantaneously expelled from macropores when the specimen is compressed, i.e. the secondary compression stage of Specimen D became observable almost immediately after each loading. Data points represented by red circles (\circ) indicate that the creep compression starts well before the time when the primary compression is completed in conventional oedometer tests.

To estimate the magnitude of instantaneous change in the void ratio of Specimen D immediately after applying each load increment, the test data (\circ) in Figure 2 are replotted in Figure 3. The eight solid circles in Figure 3(a) represent the void-ratio values of Specimen D at the beginning and end of each loading period. The horizontal lines starting from the solid circles in Figure 3(a) and bridging Figure 3(a) and (b) indicate the void ratio of Specimen D at the instance of applying new load increments. Seven solid red circles (\bullet) in Figure 3(b) are the crossing points of the seven red dotted lines and seven horizontal lines starting from seven data points in Figure 3(a). These seven circles (\bullet) indicate the elapsed time after load application when the compressive deformation starts increasing from zero. As observed in Figure 3(b), these seven circles (\bullet) exhibit a time shorter than 0.0004 min (0.024 s), implying that Specimen D did not experience any ‘instantaneous compression’. All the subsequent compression is creep compression, which increases linearly with the logarithm of elapsed time. Immediately after the application of the load increment at each loading stage, Specimen D does not seem to experience any instantaneous (elastic or elasto-plastic) compressive deformation, but only time-dependent (creep) compression. Here, as a preparation for constructing the theory, we define the initial time t_0 as the time when the creep compression starts to increase (red circles (\bullet) in Figure 3(b)).

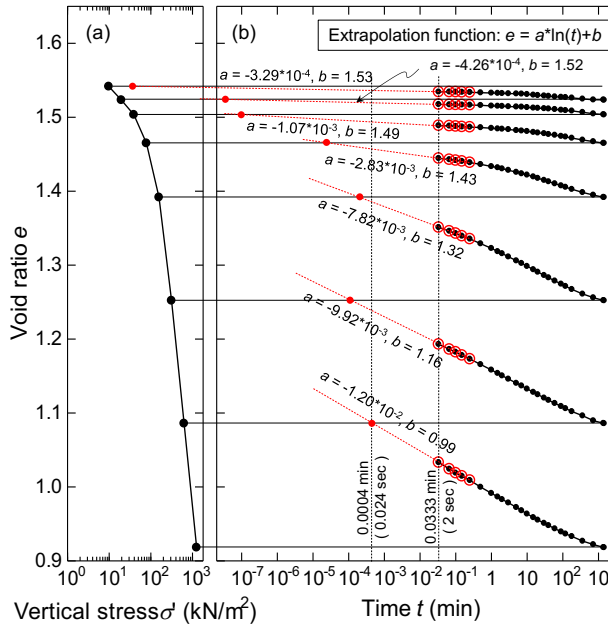


Figure 3 Extrapolation of data from oedometer test on Specimen D. (a) $e - \log \sigma'$ plots. (b) Extrapolation of $e - \log t$ curves.

3 EXPERIMENTAL EVIDENCE-II

Figure 4 shows the time-strain plots of 8 oedometer tests. 8 undisturbed clays taken from the planned area of expansion of Tokyo International Airport (Haneda Airport) are used in the tests (depth AP -16 m to -32 m, $w_n = 65.9 - 123.1\%$, $w_L = 95.0 - 130.0\%$, $w_p = 43.0 - 65.7\%$). Extrapolating 8 curves of the time-compressive strain relation observed in the secondary stage of compression, it can be seen that

- 1) 8 sets of test results indicate that creep compression starts increasing almost immediately (at time about or less than 0.006 s) after loading ($628 \rightarrow 1225 \text{ kN/m}^2$),
- 2) The compressive strain immediately after incremental loading is zero in 8 oedometer tests, implying that no instantaneous elastic (or elasto-plastic) response is experienced by 8 specimens.

These two sets of findings are essentially identical to those of Ohta et al. (2022) introduced in the previous section.

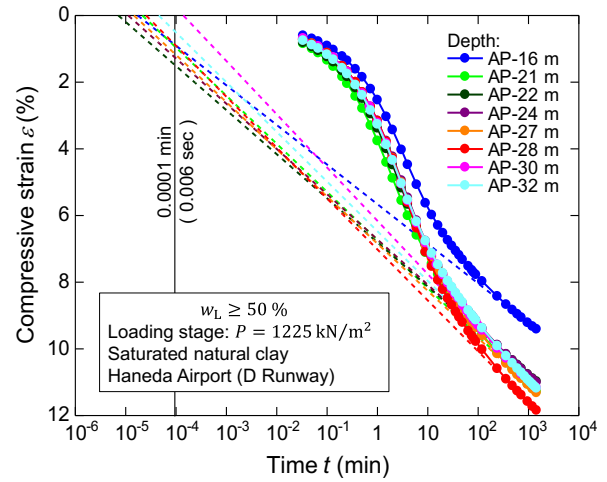


Figure 4 A new set of oedometer test data on Haneda clay (Data: Courtesy of Tokyo International Airport Construction Office, Ministry of Land, Infrastructure, Transport and Tourism)

4 DEVELOPMENT OF BASIC EQUATIONS

Based on the experimental findings introduced in the previous sections, a set of basic equations for 1-D consolidation is derived as follows. The secondary compression discussed in this study can be represented by the Voigt model. The constitutive relation of the Voigt model expressed in terms of the effective stress is $\sigma' = \eta \dot{\epsilon} + E \epsilon$, where η is the viscosity coefficient and E is the elastic modulus. As shown in Figure 3, under the constant load, the strain ϵ increased linearly with the logarithm of time: $\ln t$ ($t \geq t_0 > 0$), with the slope α (secondary consolidation coefficient). To satisfy $\dot{\epsilon} = \alpha/t$, the viscosity coefficient should be expressed as $\eta = -E t \ln(t/t_0) + t(\sigma_0/\alpha)$, where σ_0 is the initial (effective) stress at the time of t_0 . Thus, the constitutive relation can be written as $\sigma' = (1/m_v)\epsilon - (\alpha/m_v)\ln(t/t_0) + \sigma_0$, where $E = 1/m_v$. Under the assumption that the total stress σ is constant, the effective stress σ' can be expressed as $\sigma' = -p_w$, where p_w is the excess pore water pressure. Then, we get $\dot{\epsilon} = -m_v \dot{p}_w + \alpha/t$. By substituting Darcy's law and the continuity expression: $\dot{\epsilon} = -\partial[(k/\gamma_w)(\partial p_w/\partial z)]/\partial z$, the 1-D consolidation equation taking account of the secondary compression can be derived as $c_v \partial^2 p_w/\partial z^2 = \partial p_w/\partial t - \alpha/(m_v t)$, where c_v ($= k/(\gamma_w m_v)$) is the consolidation coefficient, and k , m_v , and γ_w are permeability coefficient, volumetric compression coefficient, and unit volume weight of water, respectively. The

derivation of the consolidation equation from the governing equations for the soil-water coupled field is shown in Figure 5. In Figure 6, the obtained settlement-time curves are compared with the experimental results shown in Figure 2.

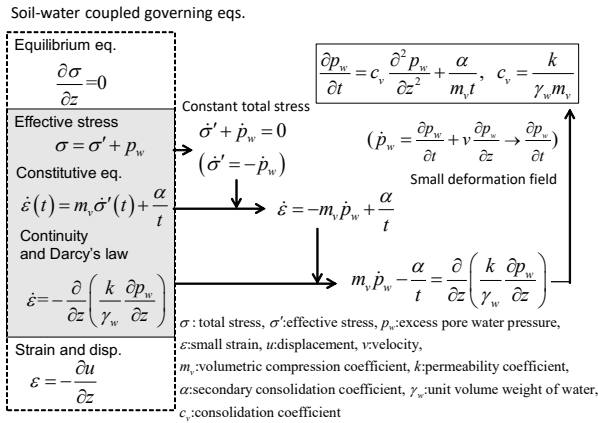


Figure 5 Derivation of 1-D consolidation model considering the secondary compression under the soil-water coupled field

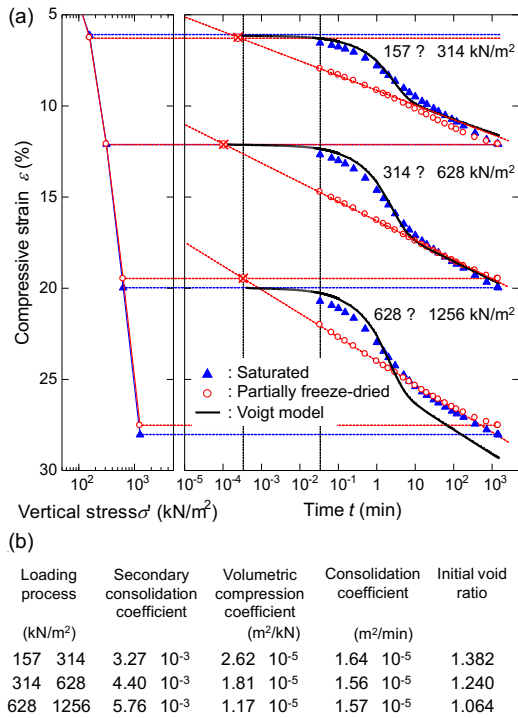


Figure 6 Comparison with the experimental results and input parameters

Assuming this constitutive relation of the Voigt model: $\sigma' = (1/m_v)\varepsilon - (\alpha/m_v)\ln(t/t_0) + \sigma_0$, Mikasa's consolidation equation (MacNabb, 1960 and Mikasa, 1963) can also be derived. Namely, substituting this constitutive equation into the equilibrium equation: $\partial \sigma / \partial z = \partial \sigma' / \partial z + \partial p_w / \partial z = 0$, and using the Darcy's law and continuity relation: $\dot{\varepsilon} = -\partial[(k/\gamma_w)(\partial p_w u / \partial z)] / \partial z$, we obtain $\partial \varepsilon / \partial t = \partial[(k/\gamma_w m_v)(\partial \varepsilon / \partial z) + (k/\gamma_w)(\partial \sigma_0 / \partial z)] / \partial z$. Furthermore, since σ_0 is constant then $\partial \sigma_0 / \partial z = 0$, we finally obtain: $\partial \varepsilon / \partial t = c_v \partial^2 \varepsilon / \partial z^2$ that is known as Mikasa's equation. Note that the assumption that the total stress is constant is not employed here. The theoretical development is summarised in Figure 7, in the same form as that shown in Figure 5. The 1-D

consolidation equation thus obtained is found to be complete as a governing equation of the boundary value problem under the soil-water coupled field.

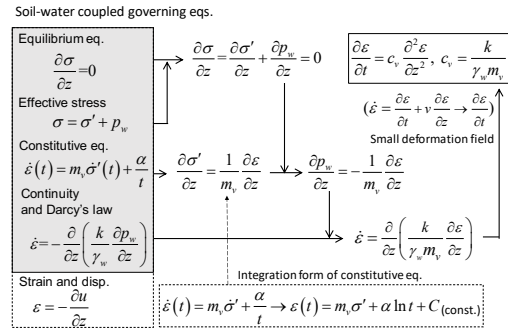


Figure 7 Derivation of 1-D consolidation model considering the secondary compression in terms of strain

5 CONCLUSIONS

A new theory for 1-D consolidation was developed based on in-depth experimental findings. Mikasa's equation was also derived from the above theory.

6 ACKNOWLEDGEMENTS

Tokyo International Airport Construction Office, Ministry of Land, Infrastructure, Transport and Tourism, Japan is acknowledged for their providing experimental data.

7 REFERENCES

- Bjerrum, L. 1967. Engineering geology of Norwegian normally-consolidated marine clays as related to settlements of buildings, Seventh Rankine Lecture, *Geotechnique* 17, 81-118.
- Den Haan, E. J. 1996. A compression model for non-brittle soft clays and peat, *Geotechnique* 46(1), 1-16.
- Hawley, J.G. and Borin, D.L. 1973. A unified theory for the consolidation of clays, *Proc. 8th Int. Conf. Soil Mech. Found. Eng., Moscow* 1(3), 107-119.
- Imai, G. 1989. A unified theory of one-dimensional consolidation with creep, *Proc. Int. Conf. Soil Mech. Found. Eng.* 1, Rio de Janeiro, 57-60.
- Ladd, C.C., Foott, R., Ishihara, K., Schlosser, F. and Poulos, H.G. 1977. Stress-deformation and strength characteristics. General Report, *Int. Conf. Soil Mech. Found. Eng.* 2, Tokyo, 421-494.
- MacNabb, A. 1960. A mathematical treatment of one-dimensional soil consolidation, *Quart. Appl. Math.* 17(4), 337-347.
- Mesri, G. and Choi, Y. K. 1985. The uniqueness of the end-of-primary (EOP) void ratio-effective stress relationship, *Proc. 11th Int. Conf. Soil Mech. Found. Eng.* 2, San Francisco, 587-590.
- Mikasa, M. 1963. Consolidation of soft clays, *Kajima Shuppankai*, (in Japanese)
- Ohta, H., Kondo, T., Hashimoto, T., Sakagami, T. and Iizuka, A. 2022. Separation of the primary and secondary consolidation of freeze-dried clay, *Proc. 20th Int. Conf. Soil Mech. Geotech. Eng.* 2, Sydney, 179-184.
- Suklje, L. 1957. The analysis of the consolidation process by the Isotaches Method, *Proc. 4th Int. Conf. Soil Mech. Found. Eng.* 1, London, 200-206.
- Taylor, D.W. and Merchant, W. 1940. A theory of clay consolidation accounting for secondary compression, *Journal of Mathematics and Physics -Massachusetts Institute of Technology-*, 19(3), 167-185.
- Taylor, D.W. 1948. Fundamentals of Soil Mechanics, Wiley International Edition, *John Wiley & Sons*, New York, London, 245.
- Yin, J.-H. and Graham, J. 1996. Elastic visco-plastic modelling of one-dimensional consolidation, *Geotechnique* 46(3), 515-527.